JOURNAL OF COMPUTATIONAL PHYSICS 71, 169–180 (1987)

Mapping from Rectangular to Harmonic Representation

W. SCHNEIDER* AND GLENN BATEMAN

Plasma Physics Laboratory, Princeton University, Princeton, New Jersey 08544

Received July 22, 1986; revised September 5, 1986

An algorithm is developed to determine the Fourier harmonics representing the level contours of a scalar function given on a rectangular grid. This method is applied to the problem of computing the flux coordinates and flux surface averages needed for $1\frac{1}{2}$D transport codes and MHD stability codes from an equilibrium flux function on a rectangular grid.

INTRODUCTION

Given the function $\psi(x, y)$ on a rectangular grid, our objective is to find the inverse functions $x(\psi, \theta)$ and $y(\psi, \theta)$. In particular, we wish to determine the coefficients $X_{cm}(\psi)$, $X_{sm}(\psi)$, $Y_{cm}(\psi)$, and $Y_{sm}(\psi)$ in the truncated Fourier series

$$\tilde{x}(\psi, \theta) = \sum_{m=0}^{M} [X_{cm}(\psi)\cos(m\theta) + X_{sm}(\psi)\sin(m\theta)] \tag{1}$$

$$\tilde{y}(\psi, \theta) = \sum_{m=0}^{M} [Y_{cm}(\psi)\cos(m\theta) + Y_{sm}(\psi)\sin(m\theta)], \tag{2}$$

such that the harmonic representations $\tilde{x}(\psi, \theta)$ and $\tilde{y}(\psi, \theta)$ most closely approximate the inverse functions $x(\psi, \theta)$ and $y(\psi, \theta)$. Once the $4M+2$ Fourier coefficients X_{cm}, X_{sm}, Y_{cm}, and Y_{sm} (not counting X_{s0} and Y_{s0}, which have no effect on $\tilde{x}$ and $\tilde{y}$) have been determined for $m = 0,..., M$, for a sufficiently dense set of ψ values within the range of interest, then $X_{cm}(\psi)$, $X_{sm}(\psi)$, $Y_{cm}(\psi)$, and $Y_{sm}(\psi)$ can be determined as needed by interpolation.

I. LEAST SQUARES FIT

The essential idea of our method is to vary the harmonic coefficients X_{cm}, X_{sm}, Y_{cm}, and Y_{sm} until a least squares fit is found for any given level contour

* Permanent address: Max-Planck-Institut für Plasmaphysik, EURATOM Ascociation, 8046 Garching bei München, Federal Republic of Germany.

0021-9991/87 $3.00

$\psi(x, y) = \Psi$. For this purpose, we choose to evaluate $\tilde{x}(\Psi, \theta)$ and $\tilde{y}(\Psi, \theta)$ at a set of at least $4M+2$ angles θ_i, $i = 1,..., I \geqslant 4M+2$. (Fewer angles and fewer harmonics are needed if any symmetry conditions are known to prevail.) If this set of angles is held fixed, the functions $\sin(m\theta_i)$ and $\cos(m\theta_i)$, $m = 0,..., M$ and $i = 1,..., I$, can be evaluated once and stored for computational efficiency. For any given value of Ψ, the coefficients X_{cm}, X_{sm}, Y_{cm}, and Y_{sm} are varied until a minimum is found for

$$W = \sum_{i=1}^{I} \{\Psi - \psi[\tilde{x}(\Psi, \theta_i), \tilde{y}(\Psi, \theta_i)]\}^2. \tag{3}$$

In Eq. (3), the Fourier series (1) and (2) are evaluated to find $\tilde{x}(\Psi, \theta_i)$ and $\tilde{y}(\Psi, \theta_i)$. Then, a two-dimensional interpolation is carried out to find $\psi(\tilde{x}, \tilde{y})$ from the values given on the rectangular grid. This process is repeated while the harmonic coefficients are varied until the function W given by Eq. (3) is minimized.

If the interpolation of $\psi(\tilde{x}, \tilde{y})$ is carried out by conventional methods (such as using piecewise polynomials), then the first and second derivatives of $\psi(\tilde{x}, \tilde{y})$ can easily be computed along with the interpolated value. In that case, we can explicitly compute smooth approximations to the first and second partial derivatives of W with respect to the harmonic coefficients with very little extra computational work. This makes the minimization of W much easier and faster.

This method should work particularly well if only a few harmonics are needed to approximate the inverse functions $x(\Psi, \theta_i)$ and $y(\Psi, \theta_i)$ to the desired accuracy. The amount of computational effort depends on the number of harmonics needed, not on the number of grid points used in the original rectangular mesh. This method also works best when a good initial guess is already in hand and only needs to be refined by further minimizing W in Eq. (3). The method works well, for example, when the level contours are changing slowly in time so that only a few iterations are needed each time the harmonics need to be updated.

II. Harmonic Optimization

One essential problem with the method described above is that the harmonic coefficients needed to minimize W (i.e., to approximate a given closed curve level contour) are not unique. The shape of each level contour is determined by $2M+3$ constraints on the harmonic coefficients, while the remaining $2M-1$ constraints, which are needed to determine all $4M+2$ harmonic coefficients, merely determine the disposition of the anglelike variable θ that parameterizes the curve. In order to see this, suppose θ is chosen to be the angle between the x axis and the tangent vector to the curve. Then

$$\frac{d\mathbf{x}}{d\theta} = \frac{ds}{d\theta}(\hat{x}\sin(\theta) + \hat{y}\cos(\theta)),$$

where s is the arclength along the curve. Now, if we expand $ds/d\theta$ as an infinite Fourier series in θ

$$\frac{ds}{d\theta} = \sum \left[S_{cn} \cos(n\theta) + S_{sm} \sin(n\theta) \right]$$

and then integrate the equation for $d\mathbf{x}/d\theta$, it can be seen that S_{c1} and S_{s1} must be zero in order to make $\mathbf{x}(\theta)$ periodic (to have the curve close on itself). If we then truncate these series for $x(\theta)$ and $y(\theta)$ to M Fourier harmonics, as in Eqs. (1) and (2), it can be seen that the following $2M+3$ coefficients

$$x_0,\ y_0,\ S_{c0},\ S_{c2},\ldots,\ S_{cM+1},\ S_{s2},\ldots,\ S_{sM+1}$$

determine the shape and position of the curve. Transforming to any other anglelike variable moves the lines of constant angle around on the curve and changes the Fourier coefficients in Eqs. (1) and (2), but leaves the shape of the curve unchanged. Note, if the curve has mirror reflection across the midplane, so that $X_{sm}=0$ and $Y_{cm}=0$ in Eqs. (1) and (2), then the shape of the curve determines $M+2$ constraints and the disposition of the anglelike variable determines $M-1$ constraints for a total of $2M+1$ coefficients.

Following the work of Hirshman and Meier [1], we establish an algorithm which minimizes the higher harmonic coefficients while leaving the shape unchanged in order to find the most rapidly converging Fourier series that approximates each level contour. This is accomplished by minimizing a penalty function P which increases rapidly with the amplitude of the highest harmonics, using only variations which leave W [defined by Eq. (3)] unchanged. An example of such a function is

$$P = \frac{\sum_{m=1}^{M} m^{p+q}(X_{cm}^2 + X_{sm}^2 + Y_{cm}^2 + Y_{sm}^2)}{\sum_{m=1}^{M} m^{p}(X_{cm}^2 + X_{sm}^2 + Y_{cm}^2 + Y_{sm}^2)}, \tag{4}$$

where p and q are positive exponents. This function reaches its absolute minimum value $P=1$ when all but the first harmonics are zero. If all the harmonics are rescaled, P remains unchanged. The zeroth harmonics X_{c0} and Y_{c0} have no effect on P, since they influence only the position and not the shape of the curve. There are many suitable functions with these properties; the particular choice made in Eq. (4) is not important. The optimum choice for exponents p and q is discussed in reference [1]. We have used $p=1$ and $q=4$ to obtain a rapidly converging harmonic representation.

The function P is to be minimized subject to the constraint that W remains unchanged. Suppose the array $\mathbf{C}=(C_1,\ldots,C_{4M+2})$ represents the set of all the harmonics being considered

$$\mathbf{C} = (X_{c0},\ldots,X_{cM},\ X_{s1},\ldots,X_{sM},\ Y_{c0},\ldots,Y_{cM},\ Y_{s1},\ldots,Y_{sM}). \tag{5}$$

Variations of **C** which leave W unchanged (and, therefore, variations which run parallel to the level contour being sought) are given by

$$\delta \mathbf{C}_{\parallel} = \delta \mathbf{C} - \frac{\nabla W \cdot \delta C}{|\nabla W|^2} \nabla W. \tag{6}$$

The variation of P subject to this constraint is then given by

$$\delta P_{\parallel} = \sum_{m=1}^{4M+2} \frac{\partial P}{\partial C_m} \delta C_{\parallel m}. \tag{7}$$

Using Eq. (6) and rearranging, we get

$$\delta P_{\parallel} = \sum_m \left[\frac{\partial P}{\partial C_m} - \frac{\sum_i (\partial W/\partial C_i)(\partial P/\partial C_i)}{\sum_j (\partial W/\partial C_j)^2} \frac{\partial W}{\partial C_m} \right] \delta C_m. \tag{8}$$

A constrained minimum, then, is achieved when $\delta P_{\parallel} = 0$ with arbitrary variations δC_m. This results in the system of equations

$$\frac{\partial P}{\partial C_m} - \frac{\sum_i (\partial W/\partial C_i)(\partial P/\partial C_i)}{\sum_j (\partial W/\partial C_j)^2} \frac{\partial W}{\partial C_m} = 0 \qquad \text{for} \quad m = 1,..., 4M+2. \tag{9}$$

These equations need to be solved together with the equations needed for the unconstrained minimization of W

$$\frac{\partial W}{\partial C_m} = 0 \qquad \text{for} \quad m = 1,..., 4M+2. \tag{10}$$

Equations (9) and (10) taken together represent $8M+4$ equations for the $4M+2$ variables in array **C**. In spite of this, however, we will now show that this combined system of equations is not overdetermined. Let

$$W_m \equiv \frac{\partial W}{\partial C_m}, \qquad P_m \equiv \frac{\partial P}{\partial C_m}, \tag{11}$$

and

$$w_m \equiv \frac{W_m}{\sqrt{\sum_{j=1}^{4M+2} W_j^2}}. \tag{12}$$

Since the values of W_m may converge to zero at different rates as we converge to a solution of Eq. (10), the values of w_m are left free (and, in general, nonzero). The constraint equations (9), which may be written

$$P_m = \sum_{i=1}^{4M+2} w_i P_i w_m, \tag{13}$$

imply

$$w_m = \frac{P_m}{\sqrt{\sum_i P_i^2}}. \tag{14}$$

As long as the values of W_m converge to zero independent of one another, the values of w_m (and, consequently, P_m) are free, and Eq. (9) imposes no constraint on P_m.

Suppose, however, there are K linearly dependent relations among the values of W_m as they converge to zero

$$\sum_{j=1}^{4M+2} a_{jk} W_j = 0 \qquad \text{for} \quad k = 1,..., K. \tag{15}$$

It then follows that

$$\sum_{j=1}^{4M+2} a_{jk} w_j = 0 \qquad \text{for} \quad k = 1,..., K$$

and, from Eq. (14),

$$\sum_{j=1}^{4M+2} a_{jk} P_j = 0 \qquad \text{for} \quad k = 1,..., K. \tag{16}$$

Hence, any linear dependence among the values of W_m, as they converge to zero, results in a corresponding linear dependence constraint on the values of P_m. Under these conditions, there would be $4M + 2 - K$ constraints from Eqs. (10) and K constraints from Eqs. (9). Consequently, there are a total of $4M + 2$ constraining equations for the $4M + 2$ unknowns.

III. Singular Value Decomposition

The well-known technique of singular value decomposition [2, 3] can be used to isolate any linear dependence among the minimizing Eqs. (10). In order to see how this is done in the present context, Taylor series expand Eq. (10)

$$\frac{\partial W(\mathbf{C})}{\partial C_m} = \frac{\partial W(\mathbf{C}^1)}{\partial C_m} + \sum_n \frac{\partial^2 W(\mathbf{C}^1)}{\partial C_m \partial C_n} (\mathbf{C} - \mathbf{C}^1)_n + \cdots, \tag{17}$$

where $\mathbf{C}^1$ is the value of $\mathbf{C}$ at the current iteration. Neglect higher order terms and do a singular value decomposition of the Hessian matrix

$$\frac{\partial^2 W}{\partial C_m \partial C_n} = \sum_j U_{mj} \sigma_j V_{jn}, \tag{18}$$

where U and V are orthogonal matrices (i.e., $U^{-1} = U^t$) and

$$\sigma_j, \qquad j = 1,..., 4M+2$$

are the singular values. Multiply Eq. (17) on the left by U^{-1} and look for conditions under which $\mathbf{C}$ is a solution to

$$\frac{\partial W(\mathbf{C})}{\partial C_m} = 0,$$

to obtain

$$\sum_m U_{jm}(\mathbf{C}^1) \frac{\partial W(\mathbf{C}^1)}{\partial C_m} = \sigma_j \sum_n V_{jn}(\mathbf{C} - \mathbf{C}^1)_n. \tag{19}$$

If all the singular values σ_j are nonzero, then none of the equations for $\partial W/\partial C_m$ are linearly independent, and there are no further constraints imposed by Eq. (9). However, if any of the singular values are zero, $\sigma_j = 0$, then

$$\sum_m U_{jm}(\mathbf{C}^1) \frac{\partial W(\mathbf{C}^1)}{\partial C_m} = 0,$$

over that range of values of $\mathbf{C}^1$ in the neighborhood of the minimum of W where we neglected higher order terms in the Taylor series (17). For each of these linear relations among the equations for W_m, it follows from Eq. (16) that there is the same linear relation among the values for P_m

$$\sum_m U_{jm}(\mathbf{C}^1) \frac{\partial P(\mathbf{C}^1)}{\partial C_m} = 0.$$

Hence, we have the following $4M+2$ equations

$$\sum_m U_{jm}(\mathbf{C}) \frac{\partial W(\mathbf{C})}{\partial C_m} = 0, \qquad \forall j \text{ st } \sigma_j \neq 0, \tag{20}$$

$$\sum_m U_{jm}(\mathbf{C}) \frac{\partial P(\mathbf{C})}{\partial C_m} = 0, \qquad \forall j \text{ st } \sigma_j = 0, \tag{21}$$

to determine the $4M+2$ elements of the array $\mathbf{C}$.

IV. Implementation

It is useful to describe the way in which the above method was implemented, in order to point out how various problems with the implementation were solved.

First, the two-dimensional array of $\psi(x, y)$ values is searched to find the minimum or maximum values of interest. These minimax grid points are tested to determine which are elliptical (true minima or maxima, referred to as o-points), and which are hyperbolic (saddle points, referred to as x-points). One elliptical point is chosen and the true position (x_0, y_0) of that minimum or maximum is found, consistent with the interpolation being used. A suitable range is found for ψ which must not include any other minimax points. Particular care must be taken to avoid hyperbolic points, since the harmonic representations (1) and (2) will not converge on contours passing through these x-points (separatrices). A set of ψ values is chosen in this range on which the coefficients of the inverse functions will be determined, working from the center to the edge.

Near the o-point, the contours are nearly elliptical, and the inverse functions can be initially approximated by

$$x \approx x_0 + x_{1s} \sin\theta + x_{1c} \cos\theta,$$

$$y \approx y_0 + y_{1s} \sin\theta + y_{1c} \cos\theta.$$

Using the representation, we can choose $y_{1c} = 0$ and choose positive values for the other coefficients in order to place the point where $\theta = 0$ on the horizontal line $y = y_0$ to the right of the minimax point. The coefficients can then be determined analytically from the polynomial approximation to $\psi(x, y)$ near the o-point. These coefficients can be used as the first iterate for the inverse functions representing the contour closest to the o-point.

As long as the function $\psi(x, y)$ is essentially parabolic near the o-point, the harmonic coefficients scale like $h^{m/2}$ where

$$h \equiv \left| \frac{\psi - \psi_{\min}}{\psi_{\max} - \psi_{\min}} \right|.$$

The scaled coefficients are extrapolated away from the o-point in order to provide the initial iterates for each successive contour, working out to the edge. If a good initial iterate is already available from previous solutions for the harmonics, then a weighted average is taken of the two.

Problems most frequently occur near the outermost contour. If this contour is located near a separatrix, the higher harmonic amplitudes increase dramatically, making the initial extrapolation and subsequent solution more difficult. Since the x-point on the separatrix contour is a saddle point, the $[\tilde{x}(\Psi, \theta_i), \tilde{y}(\Psi, \theta_i)]$ points being evaluated in Eq. (3) can inadvertently get caught on the wrong side of the saddle, with no gradient to drive it back toward the region of interest. Near such a saddle point, and also near the edge of the rectangular domain, more care needs to be taken in the choice of interpolation used to evaluate $\psi(\tilde{x}, \tilde{y})$. For these reasons, cautious methods of extrapolation and nonlinear equation solving were used, particularly for the outer contours.

If the iteration is started far from a solution, it is generally found that none of the

singular values σ_j are zero. As the iteration proceeds, however, $2M-1$ of the singular values rapidly converge to zero, so that a transition has to be made from Eq. (20) to Eq. (21) for $2M-1$ equations. This transition is made smooth by always taking these $2M-1$ equations to be a linear combination of $|\sigma_j/\sigma_1|$ times Eq. (20) plus $1-|\sigma_j/\sigma_1|$ times Eq. (21), where σ_1 is the singular value with the largest magnitude. The other singular values are found to always remain about the same order of magnitude relative to one another.

V. Jacobian and Metric Elements

Once the inverse functions (1) and (2) have been determined for a given choice of parameters ψ and θ, it is a straightforward matter to compute the Jacobian

$$\mathcal{J}(\psi, \theta) = \frac{\partial x}{\partial \psi}\frac{\partial y}{\partial \theta} - \frac{\partial x}{\partial \theta}\frac{\partial y}{\partial \psi}, \tag{22}$$

metric elements

$$g_{\psi\psi} = \left(\frac{\partial x}{\partial \psi}\right)^2 + \left(\frac{\partial y}{\partial \psi}\right)^2, \tag{23}$$

$$g_{\theta\theta} = \left(\frac{\partial x}{\partial \theta}\right)^2 + \left(\frac{\partial y}{\partial \theta}\right)^2, \tag{24}$$

$$g_{\psi\theta} = g_{\theta\psi} = \frac{\partial x}{\partial \psi}\frac{\partial x}{\partial \theta} + \frac{\partial y}{\partial \psi}\frac{\partial y}{\partial \theta}, \tag{25}$$

area,

$$A = \int^{\psi} d\psi \int_0^{2\pi} d\theta\, \mathcal{J}(\psi, \theta), \tag{26}$$

and contour integral,

$$\oint dl\, f = \int_0^{2\pi} d\theta \sqrt{(\partial x/\partial\theta)^2 + (\partial y/\partial\theta)^2}\, f(\psi, \theta). \tag{27}$$

The Fourier representation makes it particularly easy to take θ derivatives. We use cubic spline interpolation [4, 5] in ψ to find the ψ derivatives and Fast Fourier Transform [4, 5] techniques to take products and evaluate the other nonlinear functions.

For applications involving axisymmetric figures of rotation, such as tokamak equilibria [6], we wish to map from a polar coordinate system centered on the axis

of rotation (R, Y, ϕ) to a "flux coordinate system" (ψ, θ, ϕ) given the flux function $\psi(R, Y)$. Then, the Jacobian is

$$\mathcal{J}(\psi, \theta, \phi) = R\left(\frac{\partial R}{\partial \psi}\frac{\partial Y}{\partial \theta} - \frac{\partial R}{\partial \theta}\frac{\partial Y}{\partial \psi}\right), \tag{28}$$

and the volume is

$$V = 2\pi \int^{\psi} d\psi \int_0^{2\pi} d\theta\, \mathcal{J}(\psi, \theta, \phi). \tag{29}$$

VI. Applications

Two examples are shown in Figs. 1 and 2 of axisymmetric MHD equilibria that were computed in rectangular (R, Y, ϕ) coordinates and then mapped to flux coordinates using the procedure described in this report. In each case, four harmonics were used to represent the inverse functions $R(\psi, \theta)$ and $Y(\psi, \theta)$ on each of 20 level contours. It was found that using fewer than four harmonics resulted in an observable discrepancy in the shape of the outer flux surface at the tip of the bean in Fig. 1, while using more than four harmonics led to no significant further change in the plotted results or the computed flux surface averages (Jacobian or metric elements). The exponents $p = 1$ and $q = 4$ were used in Eq. (4), which resulted in rapidly converging harmonic representations.

Both of the computed flux functions $\psi(R, Y)$ for these equilibria have reflection symmetry across the midplane. This symmetry condition was used to reduce the number of harmonic coefficients needed in Eqs. (1) and (2) and also to reduce the number of angles needed to evaluate Eq. (3). For the examples presented here, 12 equally spaced angles θ_i were used in the upper half-plane. The number of angles needed depends partly on the number of harmonics used (we need at least as many angles as harmonic coefficients) and partly on the spacing needed to resolve details of the level contour shape, particularly near the x-point of a separatrix. It is important to keep in mind that the anglelike variable θ is generally not the polar angle. The harmonic optimization procedure [Eq. (4)] helps to resolve details of the level contours with the fewest harmonics and also with the fewest angles θ_i in Eq. (3). Essentially, the optimization procedure tends to force equally spaced angles θ_i to accumulate in regions where the level contour curvature is the greatest, as can be seen in both figures.

During the iteration, linearized forms of Eqs. (20) and (21) were solved using NAG [5] routines F02WCF to find the singular value decomposition and F04ARF to solve the linear equations for **C**. On the first pass through, the PBX equilibrium shown in Fig. 1 typically needed five to six iterations per flux surface while the ASDEX case shown in Fig. 2 required only three iterations for each of the inner 17 flux surfaces and up to six iterations for the outer three surfaces. On a CRAY-1 computer, this entire mapping procedure took 2.0 cpu sec for the PBX case and 1.15 cpu sec for the ASDEX case.

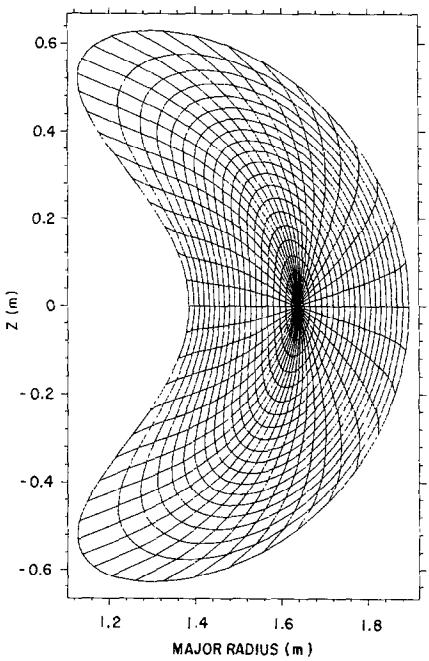

FIG. 1. Cross section of the flux coordinates computed for the Princeton Beta Experiment (PBX).

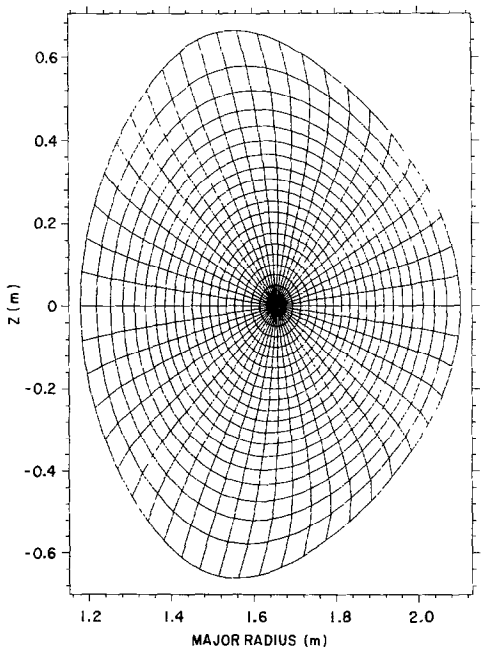

FIG. 2. Cross section of the flux coordinates computed for the ASDEX upgrade tokamak.

Clearly, the most difficult part of the computation is near the outer contours. Relative to the interval of ψ between the innermost contour and the separatrix [saddle point in $\psi(R, Y)$], the outer contour shown in Fig. 1 is 97% of the way to the separatrix. In this respect, the ASDEX case was a more difficult configuration; the outer contour shown in Fig. 2 is only 93% of the way to the separatrix.

Since the function $\psi(R, Y)$ is the solution of an elliptic equation, and consequently very smooth, for the cases presented here, sixth order polynomials in both R and Y were used to interpolate $\psi(R, Y)$ on the evenly spaced (R, Y) grid to determine the inner contours, while lower order interpolation was used near the edge. This was found to be more accurate and to use less computer memory than bicubic splines. The plasmas shown in these examples do not cover the entire rectangular grid, since other structures (limiters, walls, divertors and coils, not shown) had to also fit on the grid in the original equilibrium computations. While the entire rectangular grid in the PBX case (Fig. 1) contains 51 horizontal by 61 vertical points, there are only 14 grid points across the midplane of the plasma and 40 points from the top to bottom tips of the plasma. In the ASDEX case (Fig. 2), a 61×101 grid was used with 32×55 points between the extremities of the plasma. On of the advantages of the method presented in this paper compared to most conventional contour tracing routines is that the contours remain smooth even when the rectangular grid is coarse.

The examples described above demonstrate the capability of the method under the realistic conditions for which it was developed, but they do not provide known absolute measures with which to compare the accuracy of the results. For this purpose we computed the area enclosed by elliptical flux surfaces prescribed analytically. The results depend on the coarseness of the rectangular grid, on the method of interpolating on this grid, on the number of angles θ_i used in Eq. (3), and on the method used to integrate Eq. (26). Using a 32×32 grid, fourth order local interpolation, 20 angles θ_i, and cubic spline integration of Eq. (26) over 20 surfaces, the area was computed with relative error 4×10^{-7}.

VII. Conclusions

The method normally used to determine and integrate along level contours involves tracing out each contour by computing the local intersections of the contour as it crosses each line of the rectangular grid. Compared with this standard method, our mapping procedure has the following advantages: The computed harmonic representation is relatively insensitive to the coarseness of the rectangular grid. The mapping produces a compact parametric representation of a curvilinear coordinate system, from which the Jacobian and metric elements can be computed. The representation uses an optimal choice for the parameter θ to make the Fourier series (1) and (2) converge as rapidly as possible. Hence, this representation provides a good starting point for mapping to any other curvilinear coordinate system that follows the level contours (flux coordinates) [6]. The computational

time depends on the number of harmonics needed and the number of angles θ_i used to evaluate Eq. (3), not on the number of rectangular grid points. The iteration benefits from any previous computations, provided the contour shapes have not changed very much.

Mapping to harmonic representation in the form presented here cannot be used in multiply connected regions or in the neighborhood of a separatrix. The method must be limited to a region of simply nested level contours. When approaching a separatrix, the user must be cautious to avoid reaching out beyond the separatrix during the iteration.

When applying this method to a new problem, the user must verify that enough harmonics and evaluation angles θ_i in Eq. (3) are used. There is some incentive to choosing as few harmonics and angles as needed in order to minimize computational time. Compared to contour tracing, there is generally less interpolation on the rectangular grid, but somewhat more effort needed to compute the singular value decomposition and the solution of Eqs. (20) and (21).

ACKNOWLEDGMENTS

We wish to thank Dr. S. C. Jardin for the use of his TCS code to compute the equilibria shown in Figs. 1 and 2. We would also like to thank Dr. Michael Reusch for valuable insights during discussions. This work was supported by U.S. DOE Contract DE-AC02-76-CHO-3073.

REFERENCES

1. S. P. HIRSHMAN AND H. K. MEIER, *Phys. Fluids* **28**, 1387 (1985).
2. G. E. FORSYTHE, M. A. MALCOLM, AND C. B. MOLER, *Computer Methods for Mathematical Computations* (Prentice–Hall, Englewood Cliffs, NJ, 1977).
3. C. L. LAWSON AND R. J. HANSON, *Solving Least Squares Problems* (Prentice–Hall, Englewood Cliffs, NJ, 1974).
4. *IMSL Library User's Manual: FORTRAN Subroutines for Mathematics and Statistics* (IMSL, NBC Building, 7500 Bellaire Boulevard, Houston, Texas 77036-5085, November 1984).
5. *NAG FORTRAN Library Manual* (Numerical Algorithms Group, 1250 Grace Court, Downer's Grove, Illinois 60516, 1982).
6. G. BATEMAN, *MHD Instabilities* (M.I.T. Press, Cambridge, MA, 1978).